Journal of Physics: Conference Series **568** (2014) 022024 doi:10.1088/1742-6596/568/2/022024

# Emergence of superconductivity and magnetic ordering tuned by Fe-vacancy in alkali-metal Fe chalcogenides $Rb_xFe_{2-y}Se_2$

**Yoshiaki Kobayashi**[1,*], **Shouhei Kototani**[1], **Masayuki Itoh**[1], **Masatoshi Sato**[2]
[1] Nagoya University, Furo-cho, Chikusa-ku, Nagoya, 464-8602, Japan.
[2] Research Center for Neutron Science & Technology, Comprehensive Research Organization for Science and Society (CROSS), 162-1 Shirakata, Tokai 319-1106, Japan

*E-mail: i45323a@cc.nagoya-u.ac.jp

**Abstract**. Samples of $Rb_xFe_{2-y}Se_2$ exhibiting superconductivity [superconducting (SC) samples] undergo a phase-separation into two phases, a Fe-vacancy ordered phase with antiferromagnetic (AFM) transition at $T_{N1}$~500 K (AFM1 phase) and a phase with little Fe-vacancy and SC transition at $T_c$~30 K (SC phase). The samples of $Rb_xFe_{2-y}Se_2$ exhibiting no SC behaviour (non-SC samples) are phase-separated into three phases, the AFM1 phase, another AFM phase with $T_{N2}$ ~150 K (AFM2 phase), and a paramagnetic phase with no SC transitions (paramagnetic non-SC phase). In this paper, we present the experimental results of magnetic susceptibility, electrical resistivity, and NMR measurements on single crystals of $Rb_xFe_{2-y}Se_2$ to reveal physical properties of these co-existing phases in the SC and non-SC samples. The $^{87}$Rb and $^{77}$Se NMR spectra show that the Fe vacancy concentration is very small in the Fe planes of the SC phase, whereas the AFM2 and paramagnetic non-SC phases in non-SC samples have larger amount of Fe vacancies. The randomness induced by the Fe vacancy in the non-SC samples makes the AFM2 and paramagnetic non-SC phases insulating/semiconducting and magnetically active, resulting in the absence of the superconductivity in $Rb_xFe_{2-y}Se_2$.

## 1. Introduction

In studies on the alkali metal Fe chalcogenides $Rb_xFe_{2-y}Se_2$ with various $x$ and $y$, it is one of the intensively investigated issues to clarify the physical properties of the separated phases [1-5]. The Fe chalcogenides have two kinds of samples, one exhibiting the superconducting (SC) transition at ~30 K (SC sample) and the others with no SC transition (non-SC samples). Both kinds of the samples

commonly have the antiferromagnetic (AFM) phase with the Neel temperature $T_{N1}$ of ~500 K (AFM1 phase, the structure of space group I4/m) [3, 4]. In the SC sample, a phase with the SC transition temperature $T_c$ ~30 K (SC phase, I4/mmm) exists as another phase [1, 3, 5]. On the other hand, in the non-SC sample with the nominal ($x$, 2-$y$)=(0.7, 1.9) there are two phases besides the AFM1 phase as reported in our previous papers [3, 5, 6]. One is another AFM phase with $T_{N2}$ ~150 K (AFM2 phase, Pmna) and the other is a paramagnetic phase which has no AFM and SC transitions (paramagnetic non-SC phase, I4/mmm). However, the AFM2 phase does not always exist in the non-SC samples, suggesting that its presence sensitively depends on the concentration of the Fe-vacancy. Hereafter, non-SC samples with and without the AFM2 phase are referred as AFM2 and non-SC/non-AFM2 samples, respectively.

In this paper, we report the experimental results of magnetic susceptibility, electrical resistivity, and $^{87}$Rb and $^{77}$Se NMR measurements of these samples to elucidate clearly the physical properties of the SC, LT-AFM, and non-SC/non-AFM phases, and discuss the relationship between the electronic state and the local structure of the Fe planes in the three phases.

## 2. Experiments

$Rb_xFe_{2-y}Se_2$ single crystals were prepared by the flux method [5, 7]. The SC samples were prepared from the nominal ($x$, 2-$y$) values of (0.8, 1.7), and the AFM2 and non-SC/non-AFM2 samples were prepared from the values of (0.7, 1.9) and (1, 2), respectively. To avoid damages to the samples due to moisture or air, the samples were covered by an epoxy adhesive, Stycast 1266. In-plane electrical resistivity ρ was measured by the four terminal method with a physical property measurement system (Quantum Design, PPMS). Magnetic susceptibility χ was measured in a magnetic field $H$ of 1 (non-SC/non-AFM2 sample) or 6.105 T (SC and AFM2 samples) using a superconducting quantum interface device (SQUID) magnetometer (Quantum Design, MPMS). $^{87}$Rb NMR measurements were carried out using a coherent pulsed spectrometer and a superconducting magnet with $H$ of 6.1050 T where the single crystal was rotated using a two-axis goniometer. Fourier-transformed (FT) spectra of spin-echo signals were measured by changing the frequency stepwise and the whole $^{87}$Rb NMR spectra were obtained by superposing the FT spectra at various frequencies.

## 3. Results and Discussion

For the non-SC/non-AFM2 sample of $Rb_xFe_{2-y}Se_2$, the temperature $T$ dependences of χ for $H \perp c$ and the in-plane resistivity ρ are shown in Figs. 1(a) and 1(b), respectively, for comparison, with those of the SC and AFM2 samples [3, 5]. In the non-SC/non-AFM2 sample, the χ-increase observed for the AFM2 phase with decreasing $T$ below the AFM ordering temperature $T_{N2}$~150 K [3, 5] is suppressed, suggesting the absence of the AFM2 order. The zero resistivity observed at ~7 K for the non-SC/non-AFM2 sample is just due to the filamentary SC region, because the SC diamagnetism at $H$ =10 Oe in the zero-field-cooling condition is negligibly small. The presumed suppression of the SC transition is supported by the large electrical resistivity immediately above $T_c$ ($\rho_0$) of ~150 mΩ·cm corresponding to more than 300 times larger than the maximum metallic sheet resistance of $h/(4e^2)$~6.45 kΩ. Only the phase separation picture can consistently explain both the large $\rho_0$ and the metallic-$T$ dependence below 200 K.

Figure 2(a) shows the $^{87}$Rb NMR spectra of the SC, AFM2, and non-SC/non-AFM2 samples at 250 K for $H \parallel c$, whereas Fig. 3 presents the $^{77}$Se NMR spectrum in the SC sample. All the $^{87}$Rb NMR spectra split into a central line and two satellite lines due to the electric quadrupole interaction between the $^{87}$Rb nuclear spin $I$=3/2 and the electric field gradient at the Rb site. The expanded $^{87}$Rb NMR spectra of the central lines are also presented in Fig. 2(b). As in the case of the SC and AFM2 samples [3, 5], the spectrum of the non-SC/non-AFM2 sample is also considered to come from a paramagnetic phase in the sample, because the NMR spectrum with $H \parallel c$ coming from the AFM1 phase is wiped out by the spectrum broadening due to the magnetic order below $T_{N1}$~500 K. Thus the

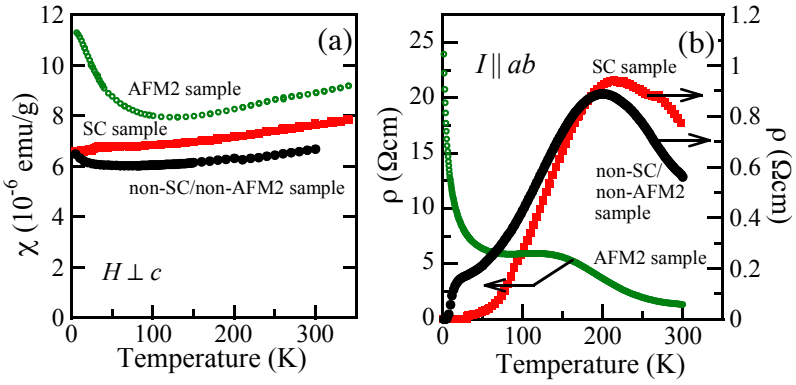


Fig. 1 Temperature dependences of (a) magnetic susceptibilities χ under a magnetic field $H \perp c$ and (b) in-plane electrical resistivities ρ of the SC, non-SC/non-AFM2, and AFM2 single crystal samples of $Rb_xFe_{2-y}Se_2$.

$^{87}$Rb NMR spectra can be calculated by assuming the $^{87}$Rb Knight shift parallel to the $c$ axis $K_c$ and the nuclear quadrupole frequency $\nu_Q$ with the electric quadrupole effect up to the second-order, its distribution $\Delta\nu_Q$, the asymmetry parameter of the electric field gradient (EFG) $\eta$ =0, and the $Z$ axis parallel to the $c$ axis. Here $\Delta\nu_Q$ is introduced, because the satellite spectra are much broadened in comparison with the central lines. By fitting the calculated spectra to the experimental ones, we obtain as $K_c$ = 0.231%, 0.236%, and 0.270%, and $\nu_Q$ = 1.74, 1.71, and 1.65 MHz, and $\Delta\nu_Q$ = 0.06, 0.12, and 0.12 MHz for the spectra of the SC, non-SC/non-AFM2, and AFM2 samples, respectively.

The results of the fitting represented by the solid curves in Fig. 2 well reproduce the central and satellite spectra in the SC sample. This NMR spectrum monitors only the SC phase as seen in Fig. 4(a) where the $^{87}$Rb Knight shift $K_c$ shows a drop due to the SC transition below $T_c$. Also it should be noted that a small FWHM of the central line showing almost no distribution in the $^{87}$Rb Knight shift. This is observed by the narrow $^{77}$Se ($I$=1/2) spectrum (Fig. 3). No distribution of the $^{87}$Rb and $^{77}$Se Knight shifts indicates that the Fe-vacancy does not exist in the Fe plane of the SC phase, consistent with its crystal structure revealed by the neutron diffraction study on the SC phase [5], whereas $\Delta\nu_Q$ monitors a distribution of Rb. Also, although the AFM1 and SC phases coexist in the the SC sample, no effects of magnetic order in the AFM1 phase on the NMR spectra of the SC phase appear as seen in Figs. 2 and 3. This fact indicates that these phases are not microscopically but macroscopically separated in the SC sample.

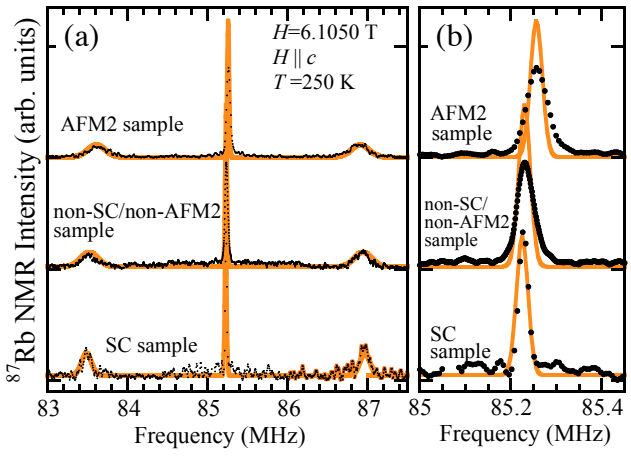


Fig. 2 (a) $^{87}$Rb NMR spectra and (b) expanded spectra of the central lines in the SC, non-SC/non-AFM2, and AFM2 samples of $Rb_xFe_{2-y}Se_2$ with $H$ (= 6.1050 T) parallel to the $c$ axis at 250 K. The solid curves represent the calculated spectra with the parameters of the Knight shift, the electric field gradient (EFG), and its distribution of EFG presented in the text.

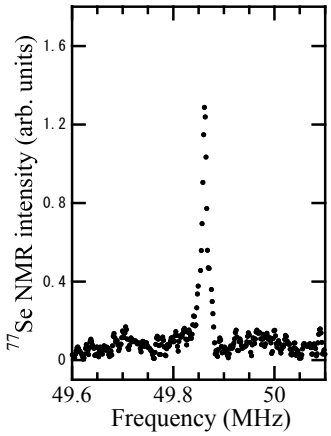


Fig. 3 $^{77}$Se NMR spectrum of the SC sample of $Rb_xFe_{2-y}Se_2$ for $H$ (= 6.1050 T) || $c$ at 250 K.

On the other hand, the fitted results for the non-SC/non-AFM2 and AFM2 samples cannot reproduce the central lines of the spectra as seen in Fig. 2(b), although they well trace the satellite lines. This discrepancy is removed by introducing a distribution of $K_c$, $\Delta K_c$, of 0.020% and 0.028% which are estimated from the FWHM of the centerlines for the non-SC/non-AFM2 and AFM2 samples, respectively. Figures 4(b) and 4(c) shows the $T$ dependences of $K_c$ with $\Delta K_c$ denoted by the vertical bars in the non-SC/non-AFM2 and AFM2 samples, respectively. A fact that the paramagnetic NMR spectrum in the AFM2 sample disappears below $T_{N2}$~150 K shows that this spectrum comes from the AFM2 phase. Thus the $T$-dependent large $K_c$ and $\Delta K_c$ in the AFM2 sample monitor the AFM properties of the AFM2 phase which may be mainly induced by a random distribution of Fe-vacancies in the Fe planes revealed by the neutron scattering study [5], whereas the $T$-independent $\Delta\nu_Q$ monitors a charge distribution due to the distributions of both Fe and Rb. This AFM2 phase is considered to have crystal and magnetic structures similar to those of a magnetic phase with $T_N$~300 K in a semiconducting sample reported in Ref. 2 and $T_N$ sensitively depends on the composition of the AFM2 phase [5]. In the non-SC/non-AFM2 sample, we observed a paramagnetic NMR spectrum, which comes from the paramagnetic non-SC phase, with $\Delta K_c$ larger than that of the SC sample and no AFM transition down to the lowest temperature measured. The large $\Delta K_c$ is ascribed to a proper amount of the disordered Fe vacancies leading to no SC and AFM transitions as reported by the neutron scattering study [5].

Thus we conclude that the SC transition in $Rb_xFe_{2-y}Se_2$ emerges in the Fe plane with almost no Fe-vacancy and disperses in the Fe plane with Fe-vacancies. The presence of Fe-vacancies activates magnetically the system and consequently suppresses the superconductivity. The emergence of the superconductivity or the magnetic orders is closely related to the absence or presence of the Fe vacancies in the Fe plane.

## 4. Conclusion

We have made magnetic susceptibility, electrical resistivity, and $^{87}$Rb and $^{77}$Se NMR measurements to elucidate the physical properties of several phases separated in the alkali metal Fe chalcogenides $Rb_xFe_{2-y}Se_2$. It was found that the system has the SC samples with the AFM1 and SC phases, the non-SC samples with the AFM1, AFM2, and paramagnetic non-SC phases, and the non-SC sample without the LT-AFM. From the analyses of the NMR spectra, we found that the SC phase has almost no Fe vacancy in the Fe plane, whereas the AFM2 and paramagnetic non-SC phases have the Fe vacancies.

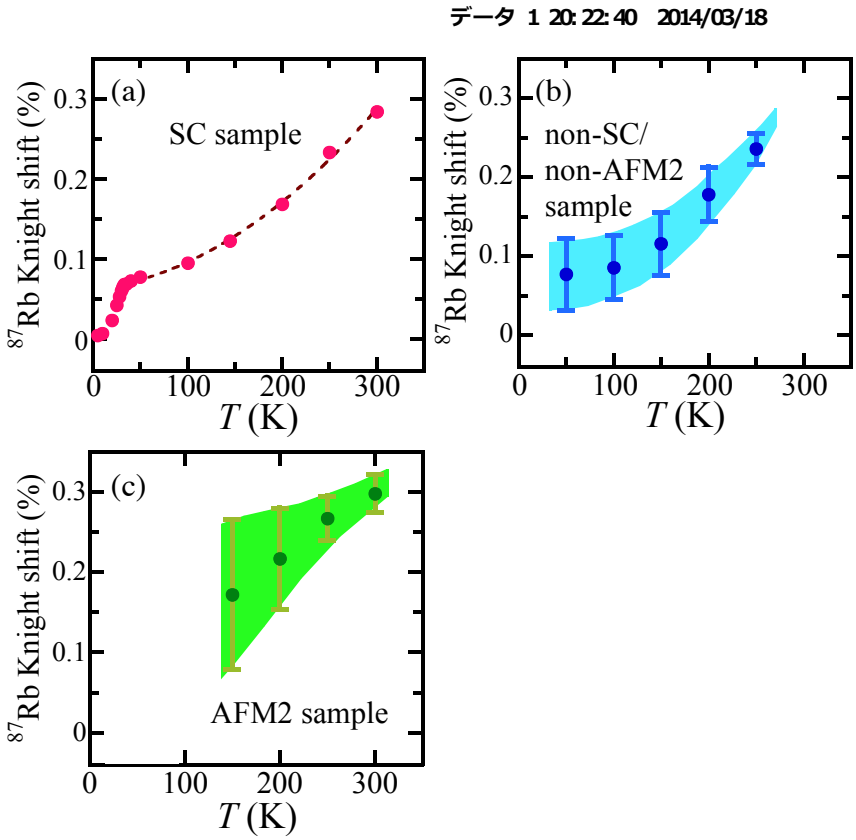


Fig. 4 Temperature dependences of the $^{87}$Rb Knight shifts for $H \parallel c$, $K_c$, in the (a) SC, (b) paramagnetic non-SC, and (c) AFM2 phases. The vertical bars indicate the distributions of $K_c$ estimated from the FWHM values of the central lines.

The magnetically active regions of the AFM2 and paramagnetic non-SC phases induced by the Fe vacancies were proposed to disperse the superconductivity.

This study was supported by the Grant-in-Aid (No. 2434080) for Scientific Research from the Japan Society of the Promotion of Science.

**References**

[1] Chen F, Xu M, Ge Q Q, Zhang Y, Ye Z R, Yang L X, Jiang Juan, Xie B P, Che R C, Zhang M, Wang A F, Chen X H, Shen D W, Hu J P, and Feng D L 2011 *Phys. Rev.* X **1** 021020
[2] Zhao J, Cao H, Bourret-Courchesne E, Lee D -H, and Birgeneau R J 2012 *Phys. Rev. Lett.* **109** 267003
[3] Kobayashi Y, Saiki S, Kototani S, Itoh M, and Sato M 2013 *J. Korean Phys. Soc.* **63** 448
[4] Bao W, Huang Q, Chen G F, Green M A, Wang D M, He J B, Wang X Q, Qiu Y 2011 *Chin. Phys. Lett.* **28** 086104
[5] Kobayashi Y, Kototani S, Kazuki Ohishi K, Itoh M, Hoshikawa A, Ishigaki T, and Sato M: submitted to *J. Phys. Soc. Jpn.*
[6] Ohishi K, Sato M, Kototani S, Saiki S, Kobayashi Y, and Itoh M 2013 *J. Korean Phys. Soc.***62** 1994
[7] Guo J, Jin S, Wang G, Wang S, Zhu K, Zhou T, He M, and Chen X 2010 *Phys. Rev.* B **82** 180520